Wearable barometric pressure sensor to improve postural transition recognition of mobility-impaired stroke patients

Masse, F ; Gonzenbach, R ; Paraschiv-Ionescu, A ; Luft, A R ; Aminian, K

Abstract: Sit-to-stand and Stand-to-sit transfers (STS) provide relevant information regarding the functional limitation of mobility-impaired patients. The characterization of STS pattern using a single trunk fixed inertial sensor has been proposed as an objective tool to assess changes in functional ability and balance due to disease. Despite significant research efforts, STS quantification remains challenging due to the high inter- and between- subject variability of this motion pattern. The present study aims to improve the performance of STS detection and classification by fusing the information from barometric pressure (BP) and inertial sensors while keeping a single sensor located at the trunk. A total number of 345 STSs were recorded from 12 post-stroke patients monitored in a semi-structured conditioned protocol. Model-based features of BP signal were combined with kinematic parameters from accelerometer and/or gyroscope and used in a logistic regression-based classifier to detect STS and then identify their types. The correct classification rate was 90.6% with full sensor (BP and inertial) configuration and 75.4% with single inertial sensor. Receiver-Operating-Characteristics analysis was carried out to characterize the robustness of the models. The results demonstrate the potential of BP sensor to improve the detection and classification of STSs when monitoring is performed unobtrusively in every-day life.

DOI: https://doi.org/10.1109/TNSRE.2016.2532844

Originally published at:
Masse, F; Gonzenbach, R; Paraschiv-Ionescu, A; Luft, A R; Aminian, K (2016). Wearable barometric pressure sensor to improve postural transition recognition of mobility-impaired stroke patients. IEEE Transactions on Neural Systems and Rehabilitation Engineering, 24(11):1210-1217.
DOI: https://doi.org/10.1109/TNSRE.2016.2532844

Wearable barometric pressure sensor to improve postural transition recognition of mobility-impaired stroke patients

F. Massé, R. Gonzenbach, A. Paraschiv-Ionescu, A.R. Luft, K. Aminian, *Member, IEEE*

***Abstract*—Sit-to-stand and Stand-to-sit transfers (STS) provide relevant information regarding the functional limitation of mobility-impaired patients. The characterization of STS pattern using a single trunk fixed inertial sensor has been proposed as an objective tool to assess changes in functional ability and balance due to disease. Despite significant research efforts, STS quantification remains challenging due to the high inter- and between- subject variability of this motion pattern. The present study aims to improve the performance of STS detection and classification by fusing the information from barometric pressure (BP) and inertial sensors while keeping a single sensor located at the trunk. A total number of 345 STSs were recorded from 12 post-stroke patients monitored in a semi-structured conditioned protocol. Model-based features of BP signal were combined with kinematic parameters from accelerometer and/or gyroscope and used in a logistic regression-based classifier to detect STS and then identify their types. The correct classification rate was 90.6% with full sensor (BP and inertial) configuration and 75.4% with single inertial sensor. Receiver-Operating-Characteristics analysis was carried out to characterize the robustness of the models. The results demonstrate the potential of BP sensor to improve the detection and classification of STSs when monitoring is performed unobtrusively every-day life.**

***Index Terms*— Postural transitions, activity monitoring, inertial sensors, barometric pressure, stroke, mobility impairments**

I. Introduction

STROKE is one of the leading cause of disability in the western world [1]. According to a survey conducted by Williams et al. [2], 66% of the stroke population suffers from mobility impairments related to balance unsteadiness, walking problems, and difficulties in transitioning between functional activities such as lying, standing and sitting [2, 3]. The daily-life monitoring of the quantity (number) and quality (e.g. slowness, smoothness) of sit-to-stand (SiSt) and stand-to-sit (StSi) transfers, one of the most physically-demanding tasks in daily life [4], provides relevant information about the functional independence [5], balance control and effectiveness of post-stroke rehabilitation programs[5]. StSi and SiSt transfers (STS) can be reliably detected using several inertial sensors (accelerometers/gyroscopes) placed on different body segments [6, 7]. However, a multiple-sensor configuration may require a long setup time, and may hinder the patient during long-term recording in daily-life. In several studies [8, 9], STSs were identified in daily-life using a single inertial sensor placed on the trunk and advanced pattern recognition algorithms based on features extracted from the kinematic signals (acceleration and angular velocity). However, for physically-impaired patients, the dynamics of STS may change due to the functional loss and/or compensatory strategies, resulting in less reproducible kinematical patterns as compared to healthy subjects. In terms of pattern recognition algorithm's performance, this translates into a limited accuracy in identifying STSs in daily-life conditions, despite good performance on a healthy control population [8]. A possible solution to increase accuracy of STS detection would be to measure the body elevation change, inherent during each STS. However, when using inertial sensors this measurement is affected by the error due to integration drift [10]. A barometric pressure (BP) sensor could provide an absolute estimate of the altitude/elevation nevertheless, there exist a number of error sources interfering with the change of body elevation, such as temperature and weather changes, or even sudden airflow. Due to these interferences, BP sensors have mostly been used in ambulatory monitoring to distinguish between different dynamic activities requiring high elevation change, e.g., level walking versus stair climbing up/down [11-14], energy expenditure estimates [15], or fall detection [16]. The focus of introducing BP in these papers was hence not on to improve STS recognition but

rather the performance of activity classification.

For application such as STS transfer monitoring, the trunk elevation change is smaller and even the best current commercial sensor for wearable monitoring applications [17] needs to operate close to its noise level (1.2 Pa / ~10cm). A recent feasibility study [17] demonstrated the suitability of using BP sensor for identifying STS involving smaller elevation change. This study presented a methodology to select a barometric pressure sensor with appropriate performance for the detection and the recognition of STS. It was focused mostly on the BP sensor evaluation and consequently has some limitations: (1) the recognition of transition type (i.e., SiSt or StSi) was carried out using the information from BP sensor only (no fusion with inertial sensors data); (2) data were collected in controlled laboratory conditions (the persons were asked to stand-up and sit-down), with relatively young participants which is known to lead to better recognition performance as compared to spontaneous real-life situations[18] and mobility impaired subjects [8]. Another study [19], carried out on babies, presented an algorithm able to distinguish non-level from level activities (climbing up and down, sitting down to the ground, and standing up on the feet) based on BP with excellent accuracy, without full analysis of sensitivity/specificity metrics or a confusion matrix. Though important as the first step of validation, a controlled laboratory measurement conditions lack ecological validity since activities are not performed in a spontaneous way. Therefore a semi-structured data collection protocol is generally recommended [18] as the second validation step, where the subject performs a series of daily activity in a natural way for at least 30 min. The scenario and environment offers different possibilities of performing an activity and the subject decides on the order and the way to carry it out.

Based on the hypothesis that the measurement of trunk elevation changes can improve the performance of STS detection and recognition, in this paper, we propose an improved method to recognize the STS patterns from inertial and BP sensors. The main aim of this study is to quantify the improvement of STS recognition when inertial sensor (accelerometers, gyroscopes) is used in combination with BP sensor. We then investigate the relevance of features extracted from each sensor to recognize STS and evaluate the performances of STS classification with mobility-impaired stroke patients monitored in a semi-structured protocol conditions.

II. Methods

This section first describes the data collection protocol carried out on a mobility-impaired stroke population. Then the wearable measurement/monitoring system, the reference system for validation, and the different features extracted from BP and inertial sensors are detailed. Furthermore, several detection and classification regression models fusing the various set of features are presented and compared.

A. ***Data collection***

Data was collected at the Kliniken Valens rehabilitation center (Valens, Switzerland), on 12 mobility-impaired stroke patients (7 Females and 5 Males / Age=59.6±13.6 y.o. / Height = 170.1±9.10 cm / Weight=73.9±14.1 kg) suffering from hemiplegia. Eight out of twelve patients were able to walk independently and four patients were walking with assistance such as a cane or a rollator.

Each patient was equipped with a set of wearable sensors and performed daily-life activities as instructed by the physician, for approximately 45 min, following a semi-structured protocol[18]. The target was to include a set of usual daily-life activities (i.e., walking along a corridor, watching TV, washing hands, eating, pouring and drinking water and, sleeping, shoe lacing, reading the newspaper, and putting on and off the jacket) involving basic body postures, locomotion and transitions between postures (i.e., walking episodes with different durations, walking up and down the stairs, taking the elevator, postural changes between lying, standing and sitting with and without arm movements). In order to verify the ability of the algorithm to recognize different STS patterns, various seats were included on the monitoring path: arm chair, bed side, sofa, armless chair, and stool. Confounding activities that involved an altitude change of the trunk such as shoe lacing or sitting on the bed after lying were also included in the protocol to further challenge the STS recognition algorithm. These activities were suggested in such a way that flexibility was given on how and when to perform the various activities. For instance, the activity "watching TV" required the patient to walk towards the TV area, sit down on the sofa, use the remote control for turning on the TV and relax while watching TV. Furthermore, the number and the order of the instructed activities were not scripted in advance. The study was approved by the ethical committee (St Gallen, Swiss Canton) and the patients signed an informed consent form prior to start collecting the data.

B. Measurement system and validation reference

During the data collection, the measurement system consisted of a small wearable sensor module (Physilog® 10D Silver, GaitUP, CH) placed on the patient at trunk (sternum) location. The system recorded to an on-board memory card the signals from a calibrated [20] inertial sensor (3D accelerometer and 3D gyroscope) at 200Hz, and from a BP sensor at 25 Hz. The precision of the BP sensor, factory-calibrated, is 1.2 Pa (~10 cm) according to the manufacturer's datasheet [21]. The signals from the accelerometer, the gyroscope and the BP sensors were first resampled at the same frequency of 40Hz to allow for faster processing. This frequency is still high enough to extract activity features [22, 23]. Moreover, the wearable sensors were aligned with the body segments by a calibration procedure based on two defined postures: lying down on a bed and standing upright against a wall. This procedure was necessary to ensure robustness against sensor misalignment across patients [24].

During the trial, each patient was videotaped and an additional wearable module (wirelessly synchronized with the trunk module) was placed on thigh. The information from the video camera and the thigh sensor formed the ground truth for the number and type of STSs (i.e., SiSt or StSi). The reason the video and the additional thigh sensor was combined for reference was the practical issue related to (1) possibility to not detect a short Si-St-Si sequence with the thigh sensor as described in [6] (2) possibility that the patient is not always in the field of view of camera given that the measurement protocol was designed in a semi-controlled conditions. For each patient *i*, All true STSs and their type (SiSt or StSi) formed the reference dataset Ω^{i}_{Ref}.

C. STS recognition algorithm

Figure 1 illustrates the main processing steps of the algorithm that takes as input the sensor data and provide as output the number and type of STSs transitions. After the functional calibration procedure described above, there are four stages in the algorithm. Considering that gyroscope has a high sensitivity to detect transition, all prospective transitions (including false STS) were selected after processing angular velocity. Then a set of altitude (BP sensor) and kinematics (inertial sensor) features were extracted for each STS candidate. In order to remove false STS, we improve the specificity of the algorithm with the "Transition Detection" stage where relevant features of STS were selected through a

logistic regression-based classifier. Finally, the type of STS (i.e., SiSt or StSi) was identified using a similar logistic-regression in the "Recognition of transition type" stage. The next sections describe in detail each stage.

1) STS Candidate extraction

Prospective candidate transitions were selected based on the value of trunk tilt angle (θ_{Trunk}). This angle was obtained from the integration of the pitch gyroscope signal filtered using the wavelet transform (Coiflet) for drift reduction [22]. Then, local peak detection was carried out to find the occurrence time ($\boldsymbol{t_{TR}}$) at which θ_{Trunk} reached a minimum below a threshold $th_{trigger}$ [9]. For each patient i this threshold $th^{i}_{trigger}$ was computed in order to maximize the sensitivity over the specificity at detecting transitions as explained in section D. The set of candidate STS for each patient was denoted $\Omega^{i}_{candidate}$.

2) STS features extraction

For each STS candidate the norm of band-pass filtered acceleration signal in the sagittal plane ($\hat{a}_{Sagittal}$) was estimated. Then, a set of kinematic features using $\hat{a}_{Sagittal}$ and θ_{Trunk} were extracted [9] as described in Figure 2 and in the first two columns in Table 1. Temporal and amplitude features from the BP signals are, however, difficult to extract due to the low signal-to-noise ratio and the influences of external perturbations [17]. To overcome this issue, the BP signal was first converted to altitude (Alt) using the barometric formula [25], then the pattern of transition was enhanced using a sinusoidal fitting model ($\boldsymbol{S_{Alt}}$) as follows:

$$S_{Alt}(t) = \Delta_{Alt} \times E\left(\frac{t - Alt_{delay}}{Alt_{duration}}\right) + Alt_{drift} \times t + Alt_{offset}$$
$$with\ E(t)\begin{cases} -1/2 & if\ t \le -1/2 \\ 1/2 \times \sin(\pi t), & if\ -1/2 < t \le 1/2 \\ +1/2 & t > 1/2 \end{cases} \quad (1)$$

The model was fitted using the "Trust-region reflective" [26] optimization algorithm, which enables the parameters to remain within predefined boundaries. The model parameters Δ_{Alt}, $Alt_{duration}$, and Alt_{offset} were set in order to smooth the BP signal and parameters Alt_{drift}, Alt_{delay} were fixed to account for the datasheet specifications of the BP sensor (MS5611-BA01, Measurement Specialties). Furthermore, the absolute elevation change ($|\Delta_{Alt}|$) and its value normalized by patient's height ($|\Delta_{Alt}|_{norm}$) were added to the features set together with the sign of Δ_{Alt} ($Sign_{\Delta\_Alt}$). An additional feature ($|\Delta_{Alt}|_{kernel}$) smoothly

binding the absolute altitude change was extracted to be more robust towards events not related to STS transitions that may combine trunk bending with an elevation shift, such as climbing up the stairs. It was computed by applying on $|\Delta_{Alt}|$ a Gaussian kernel with a mean value ($\mu_{patients}$) corresponding to the average patients' thigh length (over the population) and a standard deviation (σ_{sensor}) of twice the precision of the pressure sensor. The value of $|\Delta_{Alt}|_{kernel}$ was estimated as follows:

$$|\Delta Alt|_{kernel} = \frac{1}{\sqrt{2\pi\sigma_{sensor}^2}} e^{-\frac{\left(|Alt|-\mu_{patients}\right)^2}{2\sigma_{sensor}^2}} \quad (2)$$

The altitude features extracted from the BP sensor are illustrated in Figure 2 and described in Table I.

3) Transition detection

Table I included more than 20 features. In order to avoid over-fitting, issues only relevant parameters were selected among all features through a forward selection algorithm [27] and a logistic regression model as explained in section D. The logistic regression is a probabilistic statistical classification model that provides for each instance a bounded measure corresponding to the probability of belonging to a binary class. It was therefore selected because besides serving as an input feature for the classifier, the degree of confidence of each STS feature is valuable information to characterize the patients' functional ability in real-life environments. Moreover the most relevant features could be used further in the physical activity classifier as suggested by Salarian et al.[9].

Using a probability level (L^i_{detect}) , the probability (P_{tr}) of a transition in $\Omega^i_{candidate}$ to be a true ($P_{tr} \geq L^i_{detect}$) or false ($P_{tr} < L^i_{detect}$) transition was estimated with the Logistic Regression. During the forward feature selection process, the root mean squared error between the expected value (0 for a non-transition and 1 for a transition) and the probability predicted by the logistic regression was used as criteria to select relevant parameters: only the parameters that did not increase the root mean squared error by more than 0.5% were selected.

In order to compare the classification performances when using different sensor configurations, seven regression models were considered:

- $\mathbf{M_{all}}$ includes accelerometer, gyroscope, and BP/altitude features;
- $\mathbf{M_{gyro+BP}}$ includes gyroscope and altitude features

- $\mathbf{M_{acc+BP}}$ includes accelerometer and altitude features
- $\mathbf{M_{BP}}$ includes only altitude features
- $\mathbf{M}_{inertial}$ includes accelerometer and gyroscope features
- $\mathbf{M_{gyro}}$ includes only gyroscope features
- $\mathbf{M_{acc}}$ includes only accelerometer features

4) Recognition of Transition type

A similar approach to "Transition detection" was used for recognizing the type of transitions using the type probability level L^i_{type}. For each true detected transition, the type of transition was classified using a Logistic Regression based on the probability of being a SiSt ($P_{SiSt}>L^i_{type}$) or a StSi ($P_{StSi}>L^i_{type}$).

D. Algorithm validation

The classification performance was evaluated using a leave-one-patient-out cross-validation procedure [28]. During this procedure, the candidate transitions $\Omega_{candidate}$ were divided in *N* subsets (cross-validation folds) to be used for the training-testing procedure, *N(=12)* being the number of patients. For each cross-validation fold *i*, the candidate transitions from *N-1* patients were included in the training set ($\Omega^i_{candidate/train}$) and the remaining transitions from the one left-out patient (different for each fold) were included in the testing set ($\Omega^i_{candidate/test}$). A candidate transition was validated as a "true transition" if its occurrence time was within maximum ±1.5 seconds around an event in Ω^i_{Ref}, otherwise as "false-transitions". This time tolerance being chosen to account for possible difference between the reference time and the transition time measured from θ_{Trunk} [29]. For "Transition detection" stage the training set ($\Omega^i_{true/false/train}$) was composed of these "true transitions" and "false transitions", while for "Recognition of Transition Type" stage only "true transitions" ($\Omega^i_{true/train}$) were used.

The forward feature selection was also computed on the training set and applied on the test set.

It is worth noting that for the "Recognition of transition type" stage, the test set was also a subset of $\Omega^i_{candidate}$ ($\Omega^i_{candidate/test} \cap \Omega_{Ref}$) to be fair and independent from the detection stage.

All parameters of the STS recognition ($th^i_{trigger}$, $L^i_{dectect}$, L^i_{type}) were fixed in order to never use test data for training the classifier. $th^i_{trigger}$ was estimated in order to maximize the sensitivity (SEN) over the specificity (SPE), i.e., to allow a large number of prospective transitions to be included in the candidate

transitions set $\Omega^{i}_{candidate}$. $th^{i}_{trigger}$ was computed on the training set ($\Omega^{i}_{candidate/train}$) for each cross-validation fold as follows: the threshold was varied from -0.1 to -20 degrees and applied on the trunk flexion angle, θ_{Trunk}, to build for each fold *i* the Receiver-Operating-Characteristics (ROC) curves [30]. The extraction threshold ($th^{i}_{trigger}$) corresponded to the threshold value that reached at least 98% of the maximum SEN (to include most of the reference transitions) with a maximum SPE (to avoid a considerable amount of false transitions) in the training folds to ensure that most of the true transitions were in $\Omega^{i}_{candidate/train}$.

The probability level L^{i}_{detect} was calculated by sweeping to value between 0 and 1 on the training data ($\Omega^{i}_{true/false/train}$) and corresponded to the probability value that maximized both SEN and SPE metrics [30]. The procedure was repeated for each cross-validation fold. Similarly the probability level L^{i}_{type} was calculated on corresponding training dataset ($\Omega^{i}_{true/train}$).

All algorithms were implemented in Matlab 2013b (Mathworks, USA).

E. Model comparison

The performance of the different classification models (sensor configurations) were assessed for: (1) each stage separately (i.e., detection, recognition of STS type) using sensitivity (SEN), specificity (SPE) and ROC curves; (2) combined stages (detection and recognition) using the Correct Classification Rate (CCR) metric. To better indicate the classification performance for the group of patients, heterogeneous in terms of functional impairment, all metrics were estimated for each subject (each represents a test fold in the leave-one-patient-out cross-validation procedure) and then summarized as median ± interquartile range (IQR) instead of the mean±standard deviation. This latter is more appropriate for homogenous samples).

The ROC curves [30] were built for each model and each patient dataset (i.e. each cross-validation fold) by varying the probability level (L_{detect} and L_{type}) from 0 to 1 on the regression test outputs. The robustness of each model [31] was assessed using the AUC metric [32] representing the area covered under the ROC. The performance in terms of SEN and SPE metrics were computed at the optimal point of the ROC curve. This optimal point corresponds to the closed operating point to the ideal upper left-hand corner of the ROC plot, i.e., the point maximizing the product between SEN and SPE metrics [33].

The overall classification performance after the leave-one-patient-out cross-validation step were compared using the CCRs estimated for each patient dataset and each classifier.

III. Results

A. Candidate STS extraction

By using the reference data (video and thigh sensor), a total of 345 reference transitions (Ω_{Ref}) were extracted from the 7 hours of recordings collected on the 12 patients. Per patient, the minimum and maximum number of transitions were 14 and 50 respectively, with an average of 29 transitions, depending on the activity path the patient was undergoing. With a threshold $th^i_{trigger}$ for θ_{Trunk} ranging from -3.1 to -3.5 deg, depending on the fold, a number of 796 candidate transitions were detected and included in the set $\Omega_{candidate}$, out of which 339 were members of $\Omega_{Ref.}$ Six reference transitions were hence not captured by the extraction threshold $th^i_{trigger}$.

B. Feature selection

The forward feature selection step indicated different relevant features for detection and recognition stages. At the detection stage, for models including accelerometer features, $\hat{a}_{max}$ was mostly relevant, i.e. more than half of the folds selected $\hat{a}_{max}$ in their selected feature set. For models including gyroscope features, the most relevant features were θ_{max}, Δ_θ, and $\theta_{duration}$. With respect to the models incorporating altitude features, the most relevant were $|\Delta_{Alt}|_{kernel}$, Alt_{delay}, $Alt_{duration}$. Furthermore, in case of $\mathbf{M_{all}}$, the following features appeared in all the twelve folds as indicated in Table I: $\hat{a}_{max}$, θ_{max}, $|\Delta_{Alt}|_{kernel}$, and Alt_{delay}.

At the transition recognition stage (SiSt/StSi classification), for the regression models including the altitude features, the relevant feature was only Δ_{Alt}, regardless whether accelerometer and gyroscope features were included in the data set. When altitude features were not included, the relevant accelerometer features were $\hat{a}_{max}$, $t_{\hat{a}\_max}$, and $\hat{a}_{min}$ whereas the relevant gyroscope features were Δ_θ, θ_{max}, t_{θ_max}, t_{θ_stop}, and $\theta_{duration}$.

C. Classification performance

The performance metrics for each classification stage and the overall classification performance are provided in Table II (median± IQR).

For the STS detection, the ROC analysis indicated that the best median AUC after the cross-validation was obtained with the regression model $\mathbf{M}_{\mathbf{acc+BP}}$. The SEN and SPE were 88.8%±15.9% and 90.5%±21.6%, respectively. The regression model $\mathbf{M}_{\mathbf{all}}$, i.e. full sensor configuration, reached a lower median AUC compared to $\mathbf{M}_{\mathbf{acc+BP}}$ but a more steady one across the folds (lower IQR). Furthermore, all the regression models including accelerometer or gyroscope and BP, or accelerometer and gyroscope and BP (i.e., $\mathbf{M}_{\mathbf{acc+BP}}$, $\mathbf{M}_{\mathbf{gyro+BP}}$, $\mathbf{M}_{\mathbf{all}}$) outperformed the rest of the models in terms of AUC. This is also illustrated by the ROC curves shown in Figure 3; the $\mathbf{M}_{\mathbf{all}}$ come closer to the top left corner indicating better performance than the $\mathbf{M}_{\mathbf{inertial}}$.

Regarding the recognition of transition type (i.e., SiSt or StSi), the best regression models in terms of AUC were those including altitude features, with AUC very close to 1 (perfect separation). Furthermore, all regression models trained with the altitude features increased their performances in terms of SEN and SPE by at least 11.6% and 9.4% respectively. The variability across folds was also much lower: maximum IQR was 2.1% for altitude-featured models and minimum 12.3% for the remaining models.

In terms of overall classification rate, the best CCR after the cross-validation was obtained with the regression model $\mathbf{M}_{\mathbf{all}}$. In this case, the CCR was 90.6%±11.2% whereas when excluding the altitude features (e.g. $\mathbf{M}_{\mathbf{inertial}}$), the CCR dropped by 15.2% minimum reaching 75.4%±12.0%. Furthermore, the model $\mathbf{M}_{\mathbf{all}}$ performed better in terms of CCR for all folds with respect to. $\mathbf{M}_{\mathbf{inertial}}$..

IV. Discussion

The aim of this study was to investigate how the detection and classification of STS in daily life can be improved by using combined information from inertial and BP sensors fixed on the subject trunk (single location). For this purpose, we considered mobility-impaired stroke patients performing their natural daily activities in a semi-structured conditions while wearing the proposed trunk sensor and monitored with a reference system. Angular velocity and acceleration signals obtained from inertial sensor provided a set of candidate STSs and their associated kinematic features. The BP signal converted into altitude provided useful information related to the trunk elevation during postural transition. However, this type of sensor is inherently affected by many interfering sources and therefore

is characterized by a low signal to noise ratio. In order to overcome this issue, a sinus fitting function was applied to enhance the pattern of the altitude signal during the postural transition and to obtain a set of reliable features allowing detection and classification of STSs. After pre-selection of candidate transitions using the gyroscope, different combinations of kinematics and altitude features were used into seven regression models to detect and classify STSs based on a Logistic Regression classification tool. The improvements in terms of performance and robustness of different BP-featured models using data collected in twelve mobility-impaired stroke patients confirms the effectiveness of BP sensors to improve both detection and classification of STS during daily-life activity.

The efficiency of the proposed sensor configuration depends, however, on the signal/data processing strategy. Due to influences of external perturbations on the BP, the estimation of altitude from this sensor is critical. The signal processing developments indicated that a fitting (pattern matching and enhancement) approach can be an appropriate solution to account for environmental perturbations. The improvement of signal-to-noise ratio allowed to extract reliable features, useful at the different stages of detection and classification process. Moreover, different data processing strategies were adopted to improve the performance of the system. For example, the temporal (Alt_{delay}, $Alt_{duration}$) and amplitude ($|\Delta_{Alt}|_{kernel}$) parameters in the regression model were selected after forward feature selection to improve the detection of the transitions by using the most relevant information. Although the devised methodology was applied on a limited sample size (12 stroke patients), the patients presented different degrees of impairment and walking abilities. This challenged the processing stages and conducted to the definition of robust approaches relying on three optimal thresholds: one trunk-angle threshold ($th_{trigger}$), and two probability thresholds, L_{detect} and L_{type}. The trunk-angle threshold is related to the trunk dynamics during STS and was used to locate a potential transition namely the candidate transition. A high threshold value would tend to discard low amplitude and slow transitions and therefore would be more suitable for healthy subjects or patients with low deficit during transitions. Conversely, a low threshold value would be more suitable for patients with higher mobility deficit. Furthermore, the two probability thresholds were optimized for both the sensitivity and specificity at each cross-validation fold.

A simple functional calibration procedure was designed with only two body poses (standing straight

and lying) to have a systematic alignment of the sensor frame onto the body frame. This procedure improved the CCR metric by 0.5% for the $\mathbf{M_{all}}$. This result showed the robustness of the proposed method against slight orientation differences when affixing the sensor that might have occurred when placing the sensor. However the test-retest reliability of the classification and patterns of STS was not investigated. This would require further study with a protocol composed of imposed tasks to ensure similar conditions over the repeated test.

The improvement of all classification performance metrics for the models including altitude features demonstrate the importance of BP sensor at both stages of processing, i.e. not only for accurately distinguishing actual transition from non-transitions but also for identifying the type of transition (i.e. SiSt/StSi). For both stages, BP sensor essentially contributes to lower the inter-patient variability (lower IQR) and improve the specificity while keeping a high sensitivity, as compared to models including only the inertial features (see Table II). For detecting the transition, the model $\mathbf{M_{all}}$ reached a SEN=91.7%±14.2% and SPE=86.1%±18.1% compared to $\mathbf{M_{inertial}}$ which had SEN=93.5%±25.9% and SPE=74.0%±20.0%. At the SiSt/StSi classification stage, for models including altitude features, only the model parameter representing the (signed) change in altitude (Δ_{Alt}) consecutive to a candidate transition was selected. This feature enabled excellent performance metrics (SEN>97.0% and SPE>97.6%) and robustness (AUC>98.6%). A pattern matching-based method relying on inertial sensors only was also devised in a previous work [8] and compared with Salarian et al. on a population suffering from chronic pain. The improvements with respect to the work [9] was for this study 15.2% in terms of median CCR ($\mathbf{M_{inertial}}$ with respect to $\mathbf{M_{all}}$).

The study has also some limitations. Currently, the selected features for logistic regression and different thresholds used in this study were estimated based on the dataset collected and consequently tuned for stroke patients. For extending the approach to another population, it is therefore recommended to optimize the selected features and thresholds by collecting additional data on the study population. It is also worth noting that varying the different thresholds ($th_{trigger}$, L_{detect}, and L_{type}) has only limited impact on the performance if the these thresholds are fixed *a priori* (common across patients). For instance, the variation of $th_{trigger}$ from -3.1 to -3.5 deg (range of values obtained over different folds) has little effect on median CCR (-2.8% maximum for $\mathbf{M_{all}}$) related to a maximum decrease at the "Transition

detection" stage of SEN (-0.1% for $\mathbf{M_{all}}$) and SPE (-2.0% for $\mathbf{M_{all}}$). Similarly, varying L_{detect} and L_{type}, between [0.27;0.47] and [0.24;0.79] (corresponding to the range of L_{detect} and L_{type} values computed over the different folds) with steps of 0.01, led to decrease of median CCR of less than 2.8% for $\mathbf{M_{all}}$. Furthermore, by restricting the feature set to the features common across all patients for $\mathbf{M_{all}}$ ($\hat{a}_{max}$, θ_{max}, Δ_{Alt} ,$|\Delta_{Alt}|_{kernel}$, and Alt_{delay}), then the median CCR only decreased by 3.8%. For further study, we also propose to fix the value of $th_{trigger}$ by considering subject mobility (e.g. close to -3.1 for frail and close to -3.5 for fit subject) and consider at least the 5 features highlighted in Table I.

The performances of classification can also be improved by including post-processing steps that use information about the type of other body postures/activities (e.g. walking, lying), recognizable from available sensor data. According to previous work [9], the number of true negatives can be reduced (and SPE increased) by using simple fuzzy logic rules designed to 'correct' possible misdetections/misclassifications using information about other activities (e.g. walking and lying periods which are accurately detected from trunk-fixed inertial sensors). The methodology developed in this paper could be therefore integrated into a physical activity analysis algorithm devised to quantify the various aspects of physical functioning in daily life environment. A very interesting aspect from clinical point of view will be the reliable detection of the number of postural transitions to quantify dynamic of daily behavior [34]. Moreover, since the quantification of STS is clinically relevant, being related to the subject's functional capacity, the system could provide a set of metrics characterizing the physical performance during every-day life in various patient populations [35].

V. Conclusion

The results of this study demonstrate that a single device located on the trunk including both inertial and a BP sensor is a more reliable configuration than inertial sensor alone for long-term daily-life monitoring of mobility-impaired stroke patients. The devised algorithm for signal fitting, features extraction and classification fuses the multi-sensor information in an efficient way as illustrated by the very good performance metrics (sensitivity, specificity, and CCR). Furthermore, this dual (amplitude and temporal) modeling approach of BP is a valuable contribution to current activity recognition algorithm for dissociating daily-life activities involving larger amplitude differences [14] such as level

walking vs. stair climbing, or standing vs. taking the elevators. A possible extension of this work could be to apply a different machine learning classifiers (such as Support Vector Machine, decision trees, neural networks or naïve bayesian) as a way to potentially improve the classification results. Furthermore, the validation on an extended number of stroke patients and/or patients with other mobility-impairing clinical conditions, as for example Parkinson's disease, frail elderly, motor impaired children (e.g. cerebral palsy, neuromuscular diseases).

ACKNOWLEDGMENT

This work was partially supported by the FP7 Project REWIRE, grant 287713 of the European Union. The authors would like to thank Susanne Müller from Kliniken Valens for her precious help during the data collection.

REFERENCES

[1] J. Adamson, A. Beswick, and S. Ebrahim, "Is stroke the most common cause of disability?," *Journal of Stroke and Cerebrovascular Diseases,* vol. 13, pp. 171-177, 2004.

[2] L. S. Williams, M. Weinberger, L. E. Harris, D. O. Clark, and J. Biller, "Development of a Stroke-Specific Quality of Life Scale," *Stroke,* vol. 30, pp. 1362-1369, July 1, 1999 1999.

[3] W. H. Organization, "International classification of functioning, disability and health: ICF," 2001.

[4] A. Kralj, R. J. Jaeger, and M. Munih, "Analysis of standing up and sitting down in humans: definitions and normative data presentation," *J Biomech,* vol. 23, pp. 1123-1138, 1990.

[5] W. Janssen, J. Bussmann, R. Selles, P. Koudstaal, G. Ribbers, and H. Stam, "Recovery of the sit-to-stand movement after stroke: a longitudinal cohort study," *Neurorehabil Neural Repair,* vol. 24, pp. 763-769, 2010.

[6] A. Paraschiv-Ionescu, E. E. Buchser, B. Rutschmann, B. Najafi, and K. Aminian, "Ambulatory system for the quantitative and qualitative analysis of gait and posture in chronic pain patients treated with spinal cord stimulation," *Gait Posture,* vol. 20, pp. 113-25, Oct 2004.

[7] J. B. J. Bussmann, W. L. J. Martens, J. H. M. Tulen, F. C. Schasfoort, H. J. G. Berg-Emons, and H. J. Stam, "Measuring daily behavior using ambulatory accelerometry: The Activity Monitor," *Behavior Research Methods, Instruments, & Computers,* vol. 33, pp. 349-356, August 2001 2001.

[8] R. Ganea, A. Paraschiv-Ionescu, and K. Aminian, "Detection and classification of postural transitions in real-world conditions," *IEEE Trans Neural Syst Rehabil Eng,* vol. PP, Jun 6 2012.

[9] A. Salarian, H. Russmann, F. J. G. Vingerhoets, P. R. Burkhard, and K. Aminian, "Ambulatory Monitoring of Physical Activities in Patients With Parkinson's Disease," *Biomedical Engineering, IEEE Transactions on,* vol. 54, pp. 2296-2299, 2007.

[10] M. Tanigawa, H. Luinge, L. Schipper, and P. Slycke, "Drift-free dynamic height sensor using MEMS IMU aided by MEMS pressure sensor," *Proceedings of 5th Workshop on Positioning, Navigation and Communication, 2008. WPNC 2008. ,* pp. 191-196, 27-27 March 2008 2008.

[11] K. Sagawa, T. Ishihara, A. Ina, and H. Inooka, "Classification of human moving patterns using air pressure and acceleration," *Proceedings of the 24th Annual Conference of the IEEE Industrial Electronics Society, 1998. IECON '98.,* vol. 2, pp. 1214-1219 vol.2, 31 Aug-4 Sep 1998 1998.

[12] T. Fujita, K. Masaki, F. Suzuki, and K. Maenaka, "Wireless MEMS Sensing System for Human Activity Monitoring," in *Complex Medical Engineering, 2007. CME 2007. IEEE/ICME International Conference on*, 2007, pp. 416-420.

[13] B. D. R. Michael, W. Kejia, W. Jingjing, L. Ying, B. Matthew, D. Kim*, et al.*, "A comparison of activity classification in younger and older cohorts using a smartphone," *Physiological Measurement,* vol. 35, p. 2269, 2014.

[14] A. Moncada-Torres, K. Leuenberger, R. Gonzenbach, A. Luft, and R. Gassert, "Activity classification based on inertial and barometric pressure sensors at different anatomical locations," *Physiological Measurement,* vol. 35, p. 1245, 2014.

[15] J. Wang, J. R. Stephen, M. Voleno, M. R. Narayanan, N. Wang, S. Cerutti*, et al.*, "Energy expenditure estimation during normal ambulation using triaxial accelerometry and barometric pressure," *Physiological Measurement,* vol. 33, p. 1811, 2012.

[16] F. Bianchi, S. J. Redmond, M. R. Narayanan, S. Cerutti, and N. H. Lovell, "Barometric Pressure and Triaxial Accelerometry-Based Falls Event Detection," *Neural Systems and Rehabilitation Engineering, IEEE Transactions on,* vol. 18, pp. 619-627, 2010.

[17] F. Massé, A. K. Bourke, J. Chardonnens, A. Paraschiv-Ionescu, and K. Aminian, "Suitability of commercial barometric pressure sensors to distinguish sitting and standing activities for wearable monitoring," *Med Eng Phys,* vol. 36, pp. 739-44, Jun 2014.

[18] U. Lindemann, W. Zijlstra, K. Aminian, S. Chastin, E. de Bruin, J. Helbostad*, et al.*, "Recommendations for Standardizing Validation Procedures Assessing Physical Activity of Older Persons by Monitoring Body Postures and Movements," *Sensors,* vol. 14, p. 1267, 2014.

[19] Y. Nam and J. W. Park, "Child Activity Recognition Based on Cooperative Fusion Model of a Triaxial Accelerometer and a Barometric Pressure Sensor," *Biomedical and Health Informatics, IEEE Journal of,* vol. PP, pp. 1-1, 2013.

[20] F. Ferraris, U. Grimaldi, and M. Parvis, "Procedure for effortless in-field calibration of three-axial rate gyro and accelerometers," *Sensors and Materials,* vol. 7, pp. 311-330, 1995.

[21] GaitUP. Available: www.gaitup.ch

[22] B. Najafi, K. Aminian, F. Loew, Y. Blanc, and P. A. Robert, "Measurement of stand-sit and sit-stand transitions using a miniature gyroscope and its application in fall risk evaluation in the elderly," *Biomedical Engineering, IEEE Transactions on,* vol. 49, pp. 843-851, 2002.

[23] A. Salarian, H. Russmann, F. J. G. Vingerhoets, C. Dehollain, Y. Blanc, P. R. Burkhard*, et al.*, "Gait assessment in Parkinson's disease: toward an ambulatory system for long-term monitoring," *Biomedical Engineering, IEEE Transactions on,* vol. 51, pp. 1434-1443, 2004.

[24] J. Favre, B. Jolles, O. Siegrist, and K. Aminian, "Quaternion-based fusion of gyroscopes and accelerometers to improve 3D angle measurement," *Electronics Letters,* vol. 42, pp. 612-614, 2006.

[25] M. N. Berberan-Santos, E. N. Bodunov, and L. Pogliani, "On the barometric formula," *American Journal of Physics,* vol. 65, pp. 404-412, 1997.

[26] T. F. Coleman and Y. Li, "On the Convergence of Reflective Newton Methods for Large-Scale Nonlinear Minimization Subject to Bounds," *Mathematical Programming,* vol. 67, pp. 189-224, 1994.

[27] A. Jain and D. Zongker, "Feature selection: Evaluation, application, and small sample performance," *Pattern Analysis and Machine Intelligence, IEEE Transactions on,* vol. 19, pp. 153-158, 1997.

[28] B. Ripley, "Pattern recognition and neural networks, 1996," *Cambridge Uni. Press, Cambridge*.

[29] W. G. Janssen, J. B. Bussmann, H. L. Horemans, and H. J. Stam, "Validity of accelerometry in assessing the duration of the sit-to-stand movement," *Med Biol Eng Comput,* vol. 46, pp. 879-887, 2008.

[30] M. H. Zweig and G. Campbell, "Receiver-operating characteristic (ROC) plots: a fundamental evaluation tool in clinical medicine," *Clin Chem,* vol. 39, pp. 561-77, Apr 1993.

[31] S. Rosset, "Model selection via the AUC," presented at the Proceedings of the twenty-first international conference on Machine learning, Banff, Alberta, Canada, 2004.

[32] A. P. Bradley, "The use of the area under the ROC curve in the evaluation of machine learning algorithms," *Pattern recognition,* vol. 30, pp. 1145-1159, 1997.

[33] A. R. Van Erkel and P. M. T. Pattynama, "Receiver operating characteristic (ROC) analysis: basic principles and applications in radiology," *European Journal of radiology,* vol. 27, pp. 88-94, 1998.

[34] A. Paraschiv-Ionescu, E. Buchser, and K. Aminian, "Unraveling dynamics of human physical activity patterns in chronic pain conditions," *Sci. Rep.,* vol. 3, 2013.

[35] R. Ganea, A. Paraschiv-Ionescu, C. Büla, S. Rochat, and K. Aminian, "Multi-parametric evaluation of sit-to-stand and stand-to-sit transitions in elderly people," *Medical engineering & physics,* vol. 33, pp. 1086-1093, 2011.

TABLE I

THE LIST OF FEATURES DEFINED TO CHARACTERIZE THE SIGNAL PATTERN IN THE VICINITY OF OCCURRENCE TIME OF CANDIDATE TRANSITIONS. EXAMPLE OF INERTIAL AND ALTITUDE FEATURES ARE DISPLAYED IN FIGURE 2 (A) AND (B). THE FEATURES IN BOLD ($\hat{a}_{max}$, θ_{max}, $|\Delta_{Alt}|_{kernel}$, AND Alt_{delay}) AND IN ITALIC (Δ_{Alt}) WERE SELECTED IN ALL THE CROSS-VALIDATION FOLDS (PATIENTS) FOR RESPECTIVELY STS DETECTION AND STS RECOGNITION USING BP AND INERTIAL SENSORS.

Accelerometer features		**Gyroscope features**		**Altitude features**	
Name	*Definition*	*Name*	*Definition*	*Name*	*Definition*
$\Delta_{\hat{a}}$	Range of $\hat{\mathbf{a}}_{\mathbf{Sagittal}}$	Δ_{θ}	Range of θ_{Trunk}	Δ_{Alt}	*Elevation change during transition*
$\hat{\mathbf{a}}_{\mathbf{max}}$	**Maximum of $\hat{a}_{Sagittal}$**	$\boldsymbol{\theta}_{\mathbf{max}}$	**Maximum of θ_{Trunk}**	Alt_{offset}	Offset from mean value around t_{TR}
$t_{\hat{a}\_max}$	Time of $\hat{a}_{max}$	t_{θ_max}	Time of θ_{max}	$\mathbf{Alt_{delay}}$	**Delay from the center of the fit to t_{TR}**
$\hat{a}_{min}$	Minimum of $\hat{\mathbf{a}}_{\mathbf{Sagittal}}$	θ_{min}	Minimum of $\boldsymbol{\theta}_{\mathbf{Trunk}}$	$Alt_{duration}$	Duration computed from the Alt
$t_{\hat{a}\_min}$	Time of $\hat{a}_{min}$	t_{θ_min}	Time of θ_{min}	Alt_{drift}	Local drift of the altitude
		t_{θ_start}	Start of transition	$Sign_{\Delta\_Alt}$	Sign of Δ_{Alt}
		t_{θ_stop}	Stop of transition	$\lvert\Delta_{Alt}\rvert$	Absolute value of Δ_{Alt}
		$\theta_{duration}$	$t_{\theta\_stop} - t_{\theta\_start}$	$\lvert\Delta_{Alt}\rvert_{norm}$	$\lvert\Delta_{Alt}\rvert$ normalized by patient's height
				$\mathbf{\lvert\Delta_{Alt}\rvert_{kernel}}$	**Gaussian kernel value of $\lvert\Delta_{Alt}\rvert$**

TABLE II.

CLASSIFICATION PERFORMANCE. SEN (SENSITIVITY), SPE (SPECIFICITY) AND CCR (CORRECT CLASSIFICATION RATE).

METRICS ARE COMPUTER ACROSS FOLDS (MEDIAN±IQRAND)EXPRESSED IN PERCENTAGE

Model	**STS Detection**			**SiSt/StSi classification**			**Overall**
	SEN (%)	***SPE(%)***	***AUC***	***SEN(%)***	***SPE(%)***	***AUC***	***CCR(%)***
$\mathbf{M_{all}}$	91.7±14.2	86.1±18.1	93.9±8.2	100.0±0.0	100.0±2.1	100.0±1.5	90.6±11.2
$\mathbf{M_{gyro+BP}}$	95.6±8.7	86.1±23.5	93.7±11.2	100.0±1.9	100.0±0.0	100.0±0.9	90.4±15.0
$\mathbf{M_{acc+BP}}$	88.8±15.9	90.5±21.6	95.3±11.8	100.0±1.9	100.0±0.0	100.0±0.4	86.2±11.4
$\mathbf{M_{BP}}$	83.0±24.4	87.6±20.1	95.1±14.4	100.0±1.9	100.0±2.1	100.0±0.9	85.6±12.2
$\mathbf{M_{inertial}}$	93.5±25.9	74.0±20.0	88.2±12.9	89.2±10.7	86.2±8.3	91.7±12.3	75.4±12.0
$\mathbf{M_{gyro}}$	88.3±25.0	56.6±24.3	82.4±15.2	83.0±29.6	58.3±39.8	80.1±30.5	59.4±15.6
$\mathbf{M_{acc}}$	78.6±37.0	76.7±24.8	85.6±6.5	74.6±35.8	90.6±19.6	93.0±26.9	71.7±18.2

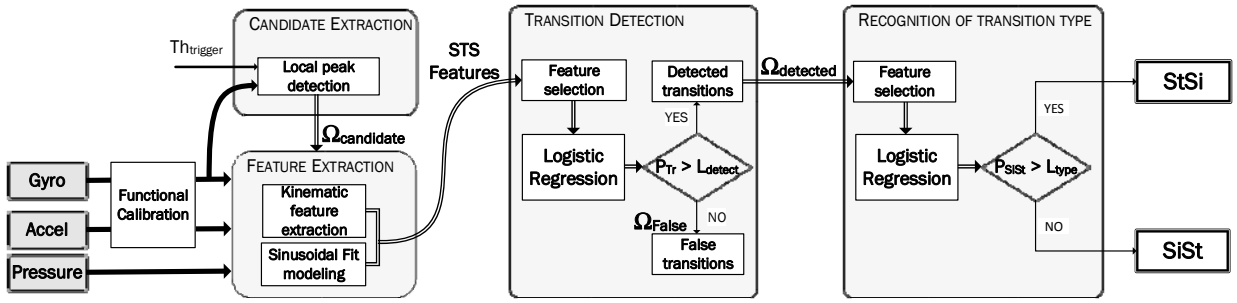

Fig. 1. Data processing flowchart: the inputs are the recorded sensor signals and the outputs is the transition type

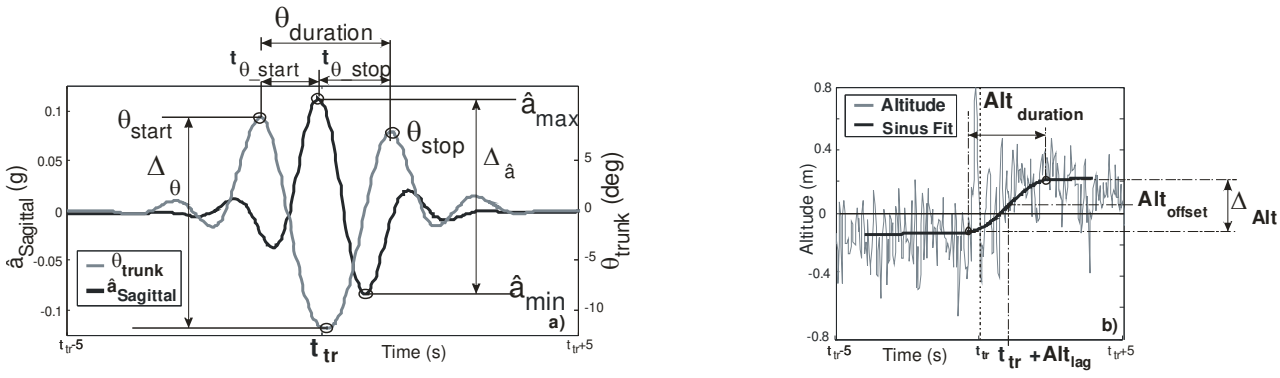

Fig. 2. Illustration of a Si-St transition pattern and the defined features extracted from the inertial signals (a) and the altitude signal (b). Panel (b) illustrates also the sinus fit model parameters that allow to enhance the pattern (altitude change) from the noisy signal during the postural change.

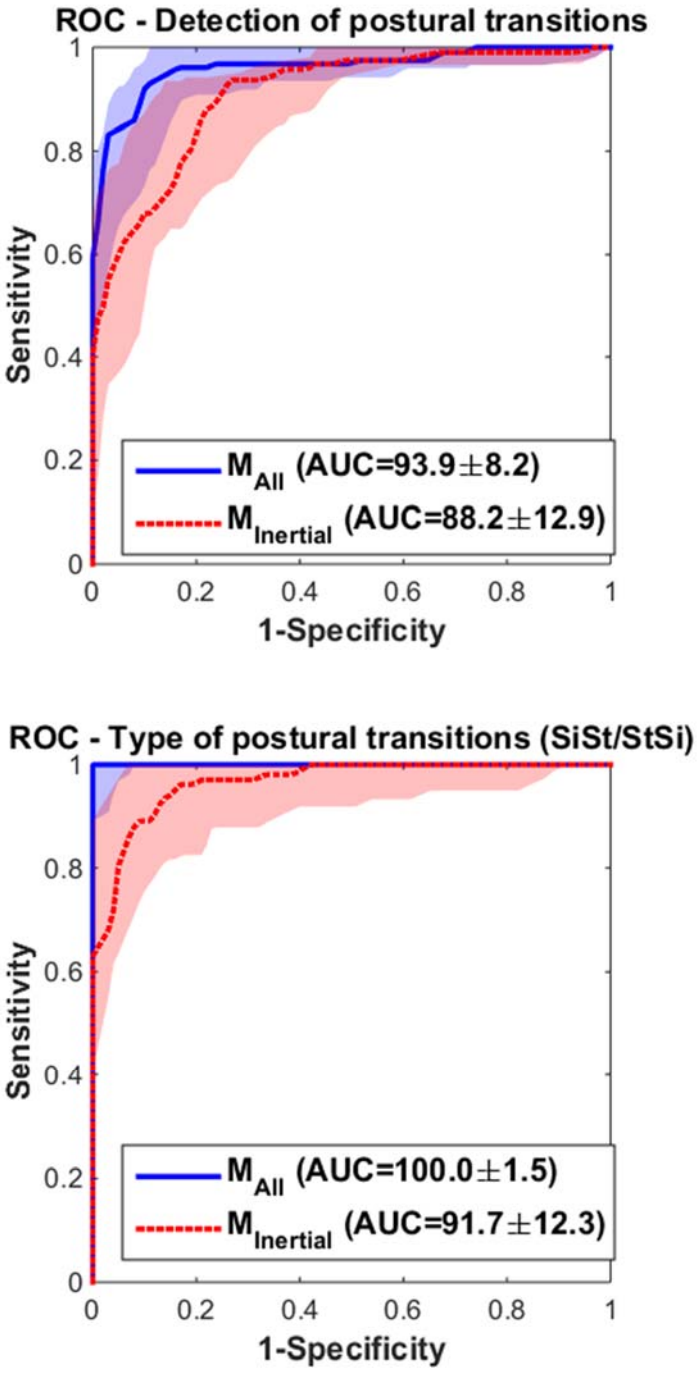

Fig 3. ROC curves of the STS detection (top) and the SiSt/StSi classification (bottom) stages. The legend is common for both plots.